



Phytogenic Synthesis, Characterisation and Multifunctional Antibacterial, Antioxidant and Anti-inflammatory Activities of Zinc Oxide Nanoparticles

B. PRATHIBHA¹, SMITHA NAIR^{2*} and V. GNANA GLORY KANMONI¹

¹Department of Chemistry and Research Centre, Women's Christian College (Affiliated to Manonmaniam Sundaranar University, Tirunelveli, India), Nagercoil-629001, India

²Department of Chemistry, Sree Ayyappa College for Women, Chunkankadai-629003, India

*Corresponding author: E-mail: smithanair@sreeayyapcollege.com

Received: 20 December 2025

Accepted: 16 February 2026

Published online: 8 April 2026

AJC-22317

In recent decades, phytochemically synthesised green nanoparticles have been extensively developed to meet a wide range of applications driven by the growing research interest in this area. Phytosynthesis of metal oxide nanoparticles was carried out using plant parts of *Artocarpus altilis* as the reducing agent. Zinc sulphate was used as the precursor, while aqueous extracts of leaves and stem bark served as the plant sources. The resulting zinc oxide nanoparticles, ZONP1 and ZONP2, were characterized using various physico-chemical techniques. SEM analysis shows large sized particles with irregular shapes as a result of agglomeration, a widely observed aspect in green synthesis. Both the nanoparticles show crystalline structures resembling standard wurtzite and their crystalline size is approximately 20 nm (XRD). From the FTIR spectra, the role of biomolecules in the formation of nanoparticles is confirmed and the UV-Vis results show a broad hump around 290-340 nm. Regarding the surface area, ZONP1 possesses a larger surface area of 14.12 m²/g, while ZONP2 has a larger pore size of 13.99 nm. ZONP1 shows a broad antibacterial spectrum while ZONP2 is active towards Gram-positive *Bacillus cereus* with an inhibition zone of 25 mm. While comparing the antioxidant capacity using the ABTS assay of ZONP1 with the larger surface area is found to show higher scavenging activity but regarding the anti-inflammatory results the ZONP2 with larger pore sizes show higher efficiency. Thus biological active chemically non-toxic environmentally safe nanoparticles are generated at minimum cost.

Keywords: Zinc oxide nanoparticles, ABTS assay, Anti-inflammatory, BET, *Artocarpus altilis*.

INTRODUCTION

The idea behind the manipulation of materials at atomic or molecular scale is always fascinating [1]. Nanoscience is an interdisciplinary field which merges biology, chemistry, physics, material science and nanotechnology allows more innovations [2,3]. Owing to its ease of preparation, minimal reaction conditions, high biocompatibility, single oxidation state, natural abundance and most important is its larger band-gap the nanoparticles of the zinc oxide are studied widely across different fields of research [4,5]. The attention of scientific community towards the metallic oxide nanoparticles is due to their significant antibacterial, antifungal [6] and anti-inflammatory activities [7,8], micronutrient and nano-fertilizer applications [1,9]. The nanoscale materials interact with the cell envelope of bacteria or fungi and degrades it causing cell death. Thus, nanoparticles with their mode of action with the

microbes creates strong antimicrobial prospects, which suppresses antimicrobial resistance [10,11].

Several synthesis approaches such as electrochemical, sonochemical, *etc.* [12] have been used since years for the manufacture and modifications of these nanoparticles depending upon their applicational area [13,14]. Among various approaches, phytosynthesis has gained attention due to the minimal chemical waste, cost-effectiveness, eco-friendly nature and enhanced biological activity compared to physically or chemically synthesized counterparts [15-17]. The advantages of green synthesised ZnO nanoparticles especially over its chemically synthesised counterparts is that they possess smaller sizes which can in turn increase their surface area and improve their photocatalytic as well as biological applications [2,18]. This surface functionality and phytochemical capping are making these particles as a biocompatible alternative [12].

Zinc plays a major role in the metabolic activities in the biological system as it is an essential trace element [19]. Hence, its oxide nanoparticles may be possibly biocompatible [11, 20-22], non-toxic and finds use in numerous applications such as cosmetics, food, textiles, medicinal, agricultural and environmental [23,24]. The accumulation of Zn²⁺ ions (from zinc oxide nanoparticles) in living cells are capable of disintegrating the microbes by generating reactive oxygen species which can cause oxidative stress and mitochondrial repair, which may ultimately lead to bacterial death [25,26] and thus act as moderate to good antimicrobials. The material possesses excellent antioxidant properties by neutralizing the free radicals and thereby reducing oxidative stress a major reason for many chronic diseases [6,27,28].

Artocarpus altilis Forsberg, belonging to the family Moraceae, is a medicinal plant [29] and its extracts are reported to be rich in flavonoids, particularly prenylated flavonoids, along with phenolic acids, sterols and fatty acids [30]. These biomolecules are known for their strong antioxidant activity due to their ability to donate hydrogen atoms or electrons and thereby stabilizing free radicals. Flavonoids, fatty acids and phytosterols such as artonin derivatives exhibit antimicrobial property by enhanced lipophilicity and membrane permeability which causes membrane disruption [31]. Also, the studies on toxicity of these plant extracts have been conducted and are found to be safe [32]. The presence of these phytochemicals may be responsible for the significant antioxidant and antibacterial activities observed in this study and also may help in the reduction of nanoparticles in green synthesis. It possesses multiple biological activities including antidiabetic, anti-inflammation, wound healing, antimalarial, antidermatitic, antisyphilitic and antiasthmatic [33,34].

Among the numerous benefits of nanoparticles is their ability to enter extracellular and intracellular spaces due to their small size which may be difficult to access for any other drug-delivery system [35-37]. Nanoparticles can prevent deterioration of drugs and thereby reduce its side effects. So, in this study the green synthesised ZnO nanoparticles, which are surface loaded with lots of active agents were studied for their possibilities as effective therapeutic agents.

EXPERIMENTAL

Zinc sulphate, sodium hydroxide, double distilled water (DD) and Whatman filter paper No.1 were supplied by Merck (India). All the chemicals were of analytical grade and used without further purification.

Sampling of plant parts: The leaves and stem bark of *A. altilis* were collected from hilly areas of Kanyakumari, India. These were verified in a taxonomic perspective at the Botany Laboratory of Sree Ayyappa College for Women, Nagercoil, India.

Extraction of plant parts: After washing two-three times thoroughly under running water, the plant parts were chopped into small fragments, dried and crushed. Each dried plant part (10 g) was placed in separate 500 mL beakers containing 250 mL of double-distilled water and boiled until the solution changed from colourless to brownish-yellow. It was filtered separately after cooling down to room temperature. The extracts

thus prepared were stored in the refrigerator for further use [38].

Synthesis of ZnO nanoparticles from *A. altilis* extract: With slight modifications to Selim *et al.*'s [39] procedure, the biogenic preparation of two samples of ZnO nanoparticles (ZONPs) was carried out. ZONP1 and ZONP2 were synthesised using leaf and stem bark extracts of *A. altilis*, respectively. About 20 mL of each extract was mixed with 2.5 g anhydrous zinc sulphate and 30 mL distilled water, followed by stirring at 80 °C with the dropwise addition of 0.1 M NaOH to adjust pH. The mixtures turned milky white (ZONP1) and off-white (ZONP2), then were stirred for 45 min, cooled, filtered, washed, dried and stored as ZnO nanoparticle powders for further analysis.

Characterisation: Biogenicity ZONP1 and ZONP2 were validated by multiple techniques including SEM/EDX, XRD, FT-IR spectroscopy, UV-Visible spectroscopy and BET. SEM/EDX to estimate the particle size and shape (Tescan, VEGA3 SBH) and for identification of elements in the phytosynthesised nanoparticles. FT-IR spectroscopy (Perkin-Elmer Spectrum 2) to confirm the presence of phytochemicals. UV-Vis spectroscopy using Shimadzu, Cary 300B10UV to study the optical properties. An XRD (Rigaku Smartlab SR) to estimate phase purity and crystallinity and BET/BJH unit using Microtrac, BELSORP-max to analyse and measure surface area and pore size of the green synthesised ZONPs.

Biological studies

Antioxidant activity assay: ABTS (2,2'-Azinobis(3-ethylbenzothiazoline-6-sulfonic acid)disodium salt) assay was used for the determination of the antioxidant potential of green synthesised ZONP1 and ZONP2 samples. ABTS stock solutions were mixed with potassium persulphate in dark at room temperature for about 12-16 h to prepare ABTS radical cation (ABTS^{•+}). It was then diluted with ethanol. By using Trolox as the standard antioxidant positive control. The free radical was mixed with Trolox as well as the samples of different concentrations. The reaction was allowed for 0.5 h at 30 °C, after which the absorbance at 734 nm was measured. Finally, the inhibition % was calculated using eqn. 1:

$$\text{Inhibition (\%)} = \frac{\text{OD}_{\text{control}} - \text{OD}_{\text{sample}}}{\text{OD}_{\text{control}}} \times 100 \quad (1)$$

Anti-inflammatory activity assay: The *in vitro* anti-inflammatory activity of ZONPs was evaluated using cyclooxygenase/lipoxygenase (COX/LOX) enzyme inhibition assays. RAW 264.7 murine macrophage cells were cultured in DMEM, stimulated with LPS (1 µg/mL) at ~60% confluence, and treated with ZONPs at 25, 50, and 100 µg/mL. COX activity was determined following Walker & Gierse's protocol [40] with absorbance measured at 632 nm, while LOX activity was assessed using Axelrod *et al.*'s method [41] with absorbance recorded at 234 nm. The percentage inhibition of COX/LOX activity [42] was determined eqn. 2:

$$\text{Inhibition of enzyme (\%)} = \frac{A_{\text{control}} - A_{\text{test}}}{A_{\text{control}}} \times 100 \quad (2)$$

Antibacterial activity assay: The antimicrobial activity of the biofabricated ZONPs was evaluated using the disc diffusion method [43] on bacteria-inoculated agar plates. Different concentrations of the samples were loaded onto discs and antimicrobial efficacy was determined by the inhibition zones against Gram-positive bacteria (*Staphylococcus aureus*, *Bacillus cereus*) and Gram-negative bacteria (*Klebsiella pneumoniae*, *Vibrio cholerae*), using ciprofloxacin (5 µg/mL) as positive control and a sterile blank disc as negative control [44].

RESULTS AND DISCUSSION

SEM/EDX studies: Scanning electron microscopy was employed for examining the interface morphology and texture of the synthesised ZnO nanoparticles. The SEM images of the ZONPs synthesised using extracts of different plant parts of *Artocarpus altilis* are shown in Fig. 1. The particles are in irregular shapes together with agglomeration. The agglomeration may be the result of high surface energy and low surface area which occurs when particle adhesion takes place through weak forces which leads to nanoentities [45]. The approximate particle sizes obtained from the SEM images were around 306 nm and 354 nm for ZONP1 and ZONP2, respectively as

shown in the images provided by the instrumentation facility (Fig. 1a-b) [46]. These values confirm the ZnO nanoparticles in the micrometer to nanometer range.

Further EDX analysis of the ZONPs show that it contains zinc and oxygen as major constituents confirming the metal oxide formation. Signals related to the carbon and sulphur were also observed. 'S' may be from the precursor concentration and 'C' may be from the associated biomolecules present in the plant which act as capping agents (Fig. 2).

XRD studies: By measuring the angle and interatomic distance between the atoms packed in a crystalline solid, it is possible to verify the structure of these materials. The XRD trend of the two zinc oxide nanoparticles synthesised from the precursor zinc sulphate and the plant extracts shows five different sharp and intense peaks. As seen in Fig. 3, the peaks are indexed with their corresponding lattice planes. The peak angles and the *hkl* values are 32.8 (100), 33.9 (002), 36.7 (101), 58.4 (110) and 69.1 (201) for ZONP1 and 33.0 (100), 34.8 (002), 37.3 (101), 58.8 (110) and 69.4 (201) for ZONP2. All these assignments were close to the standard hexagonal wurtzite, zinc oxide reflections with JCPDS: 36-1451. Some peaks are seen in both samples in the low angle region [47-49], which are likely from the organic residues in a phytosynthesis.

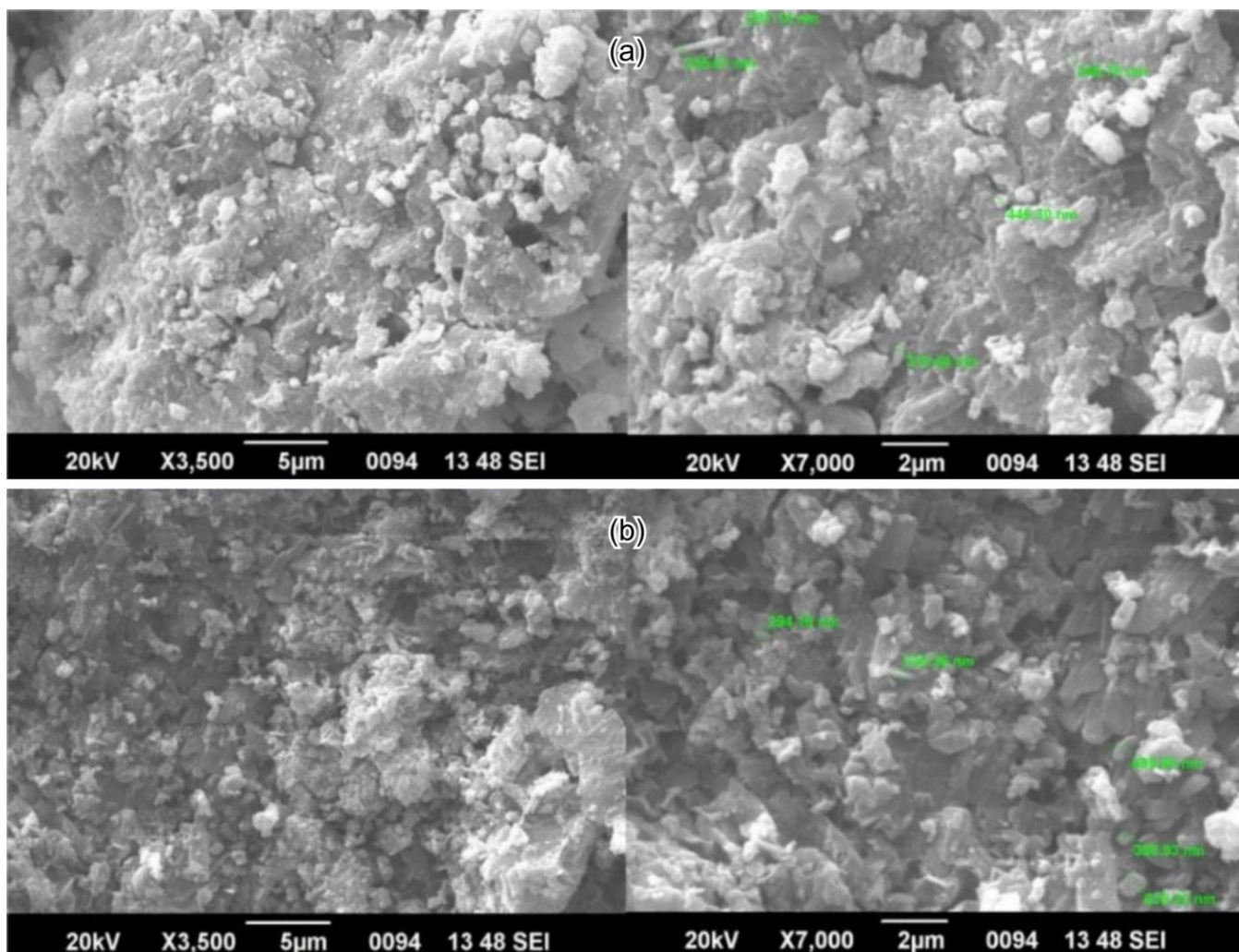


Fig. 1. SEM images of (a) ZONP1 and (b) ZONP2

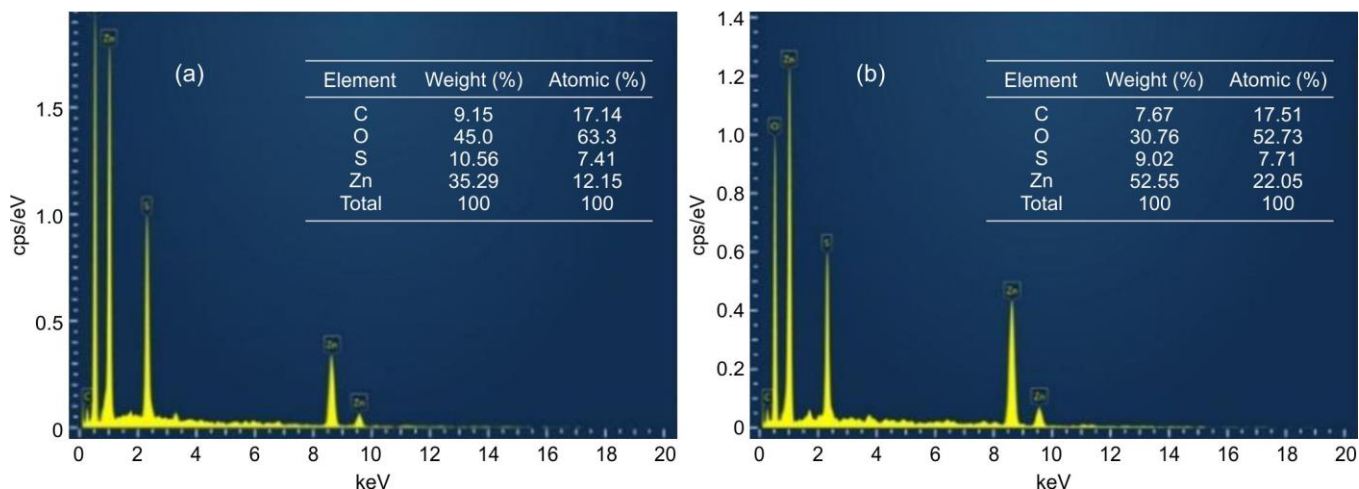


Fig. 2. EDX mapping of (a) ZONP1 and (b) ZONP2

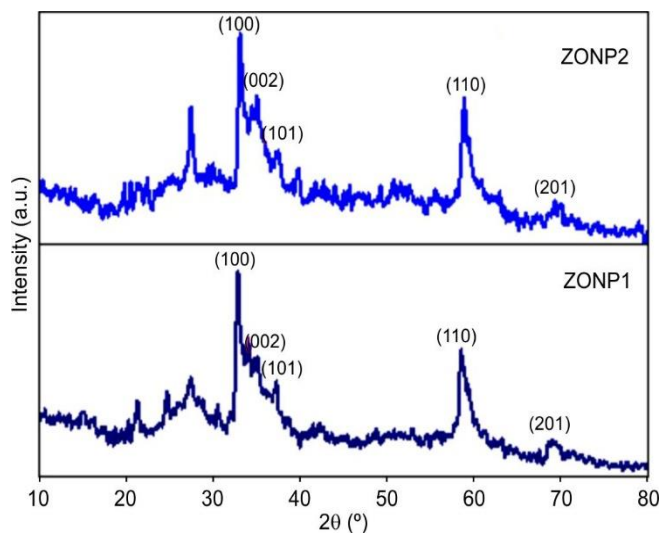


Fig. 3. XRD images of ZONP1 and ZONP2

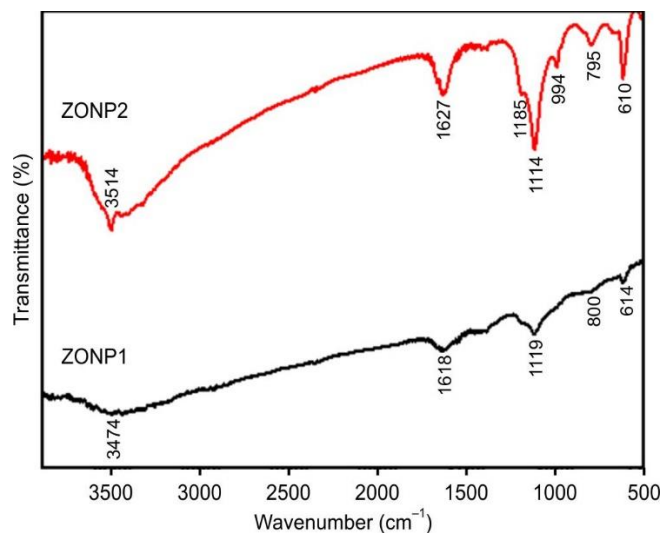


Fig. 4. FTIR spectrum of the green synthesised ZONPs

Using the Scherrer's formula [4,39], the average size of the crystallites was estimated to be approximately 19-20 nm for the two nanoparticles.

FTIR studies: The low-frequency M–O band confirming nanoparticle formation is observed at 614 cm^{-1} for ZONP1 and 610 cm^{-1} for ZONP2 (Fig. 4). The peaks around $1000\text{--}700\text{ cm}^{-1}$ always indicate out of plane C–H stretch *i.e.*, the presence of C–H bending vibrations of the aromatic ring. The presence of peaks around 800 cm^{-1} in ZONP1 and 994 cm^{-1} and 795 cm^{-1} in ZONP2 shows the presence of substituted aromatic phytochemicals. The peaks around $1200\text{--}1110\text{ cm}^{-1}$ usually show C–O, C–O–C, C–N stretches of the alcohols, ester, ether, amines, *etc.* Both the samples exhibit stretching around 1119 cm^{-1} and $1114\text{--}1185\text{ cm}^{-1}$, respectively. A peak at 1618 cm^{-1} for ZONP1 and 1627 cm^{-1} for ZONP2 may arise from C=O or C=C stretching. The broad peaks in the spectrum at 3474 cm^{-1} and 3514 cm^{-1} for these nanoparticles are due to the –OH stretching *i.e.*, mainly due to the water molecules, hydroxyl groups, *etc.* [46,50]. These results indicate that the nanoparticles are capped by hydroxyl-, amine- and amide-containing plant metabolites, where polyphenols and flavonoids act as strong reducing agents for metal ions [51].

UV-Vis: The observed colour change from colourless to light brown and finally to milky/off-white as reported by Maheo *et al.* [52], confirms successful phytofabrication, while the broad hump around 290-340 nm arises from electronic transitions (inner shell e^{-ns}) of the metal atoms during interaction of plant extracts with the precursor solution. A characteristic absorption edge in the UV-Vis spectra, near 350 nm and 349 nm for ZONP1 and ZONP2 (Fig. 5), clearly shows the presence of ZnO nanoparticles [39,53]. These results not only validate the nanoparticle formation but also evidence of the reducing and the capping ability of the polyphenols or the other active species of the plant extract. The band gap estimated for these samples using the Tauc plot method is 3.31 eV and 3.44 eV, respectively.

BET studies: From the BET experiments, the ZONPs has a BET surface area of $14.12\text{ m}^2/\text{g}$ and $6.49\text{ m}^2/\text{g}$ for ZONP1 and ZONP2, respectively and it matches well with the IUPAC classification of N_2 uptake and desorption curves (Fig. 6a&c) confirming the presence of porosity [54]. The pore volumes and pore sizes of the synthesised particles were estimated by the BJH method (Fig. 6b&d) and were found to be $0.0327\text{ cm}^3/\text{g}$ and $0.0227\text{ cm}^3/\text{g}$ and 9.26 nm and 13.99 nm, respect-

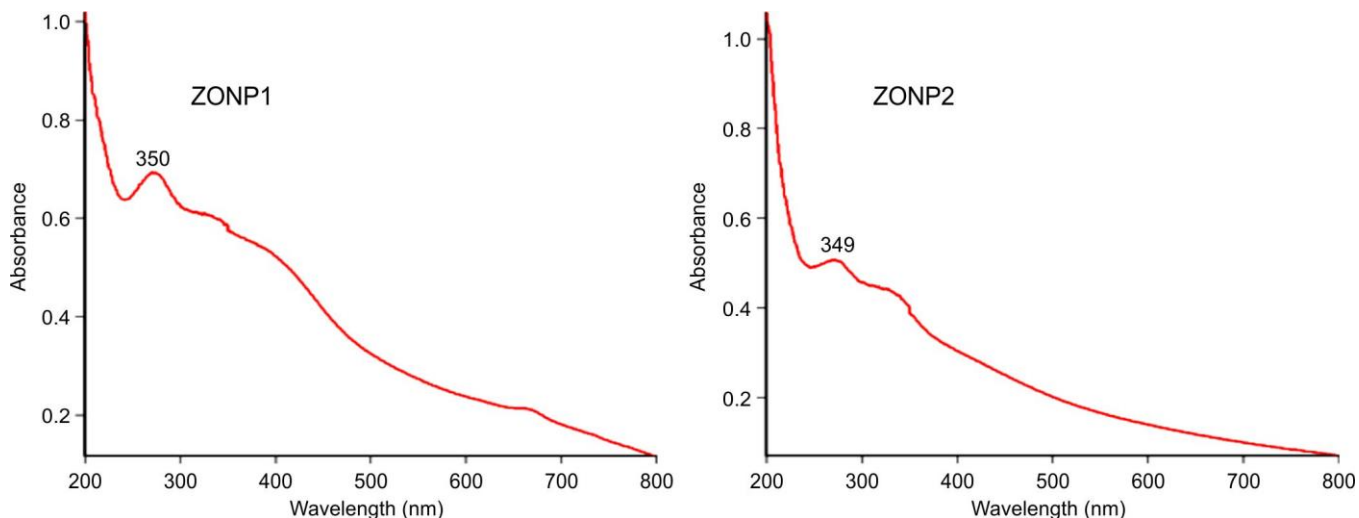


Fig. 5. UV-Vis spectra of ZONP1 and ZONP2

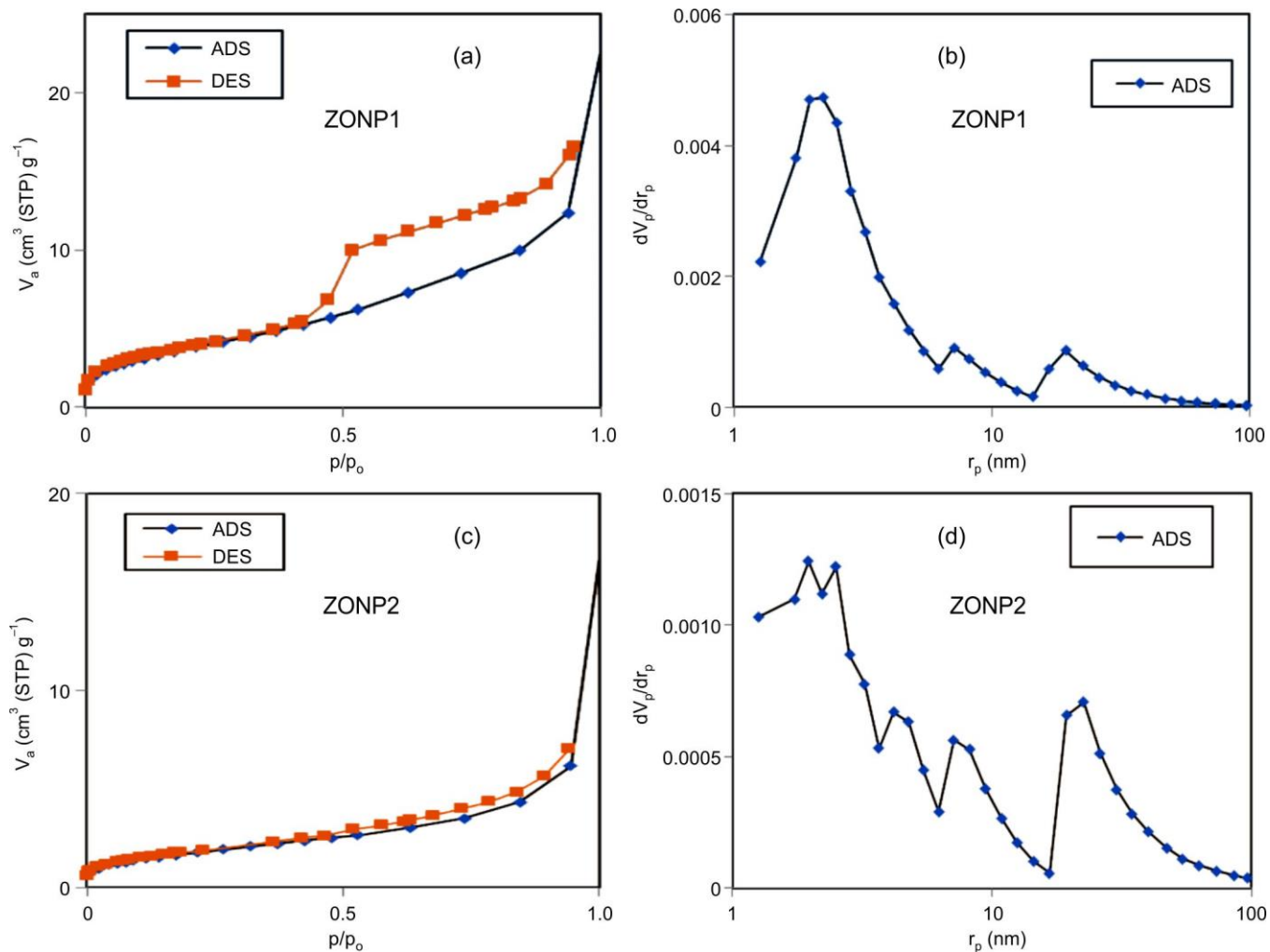


Fig. 6. N₂ adsorption-desorption isotherms (a,c) and pore size distributions (b,d) of ZONP1 and ZONP2, respectively

ively. Among the two samples, ZONP1 exhibits a comparatively larger surface area, whereas ZONP2 shows a larger pore size, with both displaying mesoporous structures. These values indicate that the zinc oxide nanoparticles can be better used for biological activities [24,55].

Anti-inflammatory activity: Comparison of the phyto-synthesized ZnO nanoparticles shows that ZONP2 exhibits stronger anti-inflammatory activity than ZONP1, with both samples demonstrating dose-dependent inhibition of COX and LOX enzymes. The IC₅₀ value of ZONP2 for COX enzyme

is 123.17 $\mu\text{g}/\text{mL}$ (against 142.42 $\mu\text{g}/\text{mL}$ for ZONP1) and 100 $\mu\text{g}/\text{mL}$ (against 116.67 $\mu\text{g}/\text{mL}$ for ZONP1) for LOX enzyme (Table-1). Even though ZONP1 has a comparatively larger surface area than ZONP2, the latter has a better pore size which might have contributed to the higher efficiency (*i.e.* ROS quenching or enzyme binding). The most important factor being the phytochemicals present in the plant which have imparted them with these qualities.

TABLE-1
ANTI-INFLAMMATORY (COX AND LOX
ACTIVITY) OF ZONP1 AND ZONP2

Sample conc. ($\mu\text{g}/\text{mL}$)	Inhibition (%)			
	COX activity		LOX activity	
	ZONP1	ZONP2	ZONP1	ZONP2
LPS	0.000	0.000	0.000	0.000
25	22.753	20.729	15.625	12.500
50	31.741	32.227	37.500	31.250
100	41.619	44.372	46.875	50.000

Antioxidant activity: In ZONPs, zinc exists in the stable +2 oxidation state and does not directly participate in redox reactions with free radicals; however, surface-bound phytochemicals such as flavonoids and polyphenols containing hydroxyl, carboxyl and aromatic groups can donate hydrogen atoms or electrons to neutralize radicals. Moreover, oxygen vacancies and the semiconductor nature of ZnO further contribute to the antioxidant activity of the ZONPs. The scavenging activity was measured for concentrations 20, 30 and 40 $\mu\text{g}/\text{mL}$. The ZONP1 has its maximum ABTS scavenging at 40 $\mu\text{g}/\text{mL}$ (57%) and minimum at 20 $\mu\text{g}/\text{mL}$ (11%) (Table-2). For the second sample the highest concentration gave a 52% scavenging activity whereas 14% was observed at its lowest concentration. The ABTS scavenging activity of these nanoparticles showed a dose dependent increase. Thus, the sample ZONP1 is having greater antioxidant activity with an IC_{50}

TABLE-2
ANTIOXIDANT ACTIVITY
(ABTS SCAVENGING) OF ZONP1 AND ZONP2

Conc. ($\mu\text{g}/\text{mL}$)	Inhibition (%) of ABTS scavenging		
	ZONP1	ZONP2	Standard (ascorbic acid)
20	11.145 \pm 0.156	14.031 \pm 0.079	34.892 \pm 0.018
30	32.152 \pm 0.064	27.576 \pm 0.024	43.317 \pm 0.015
40	56.597 \pm 0.024	52.431 \pm 0.214	65.889 \pm 0.515
IC_{50} value	37.3493	40.944	31.269

TABLE-3
ANTIBACTERIAL ACTIVITY OF ZONP1 AND ZONP2

Concentration	Inhibition zone diameter (mm)							
	Gram-positive				Gram-negative			
	<i>B. cereus</i>		<i>S. aureus</i>		<i>K. pneumoniae</i>		<i>V. cholerae</i>	
	ZONP1	ZONP2	ZONP1	ZONP2	ZONP1	ZONP2	ZONP1	ZONP2
250 $\mu\text{g}/\text{mL}$	11	17	7	9	9	8	9	8
500 $\mu\text{g}/\text{mL}$	16	20	10	11	11	10	14	11
1 mg/mL	17	25	12	13	16	13	16	14
PC	33	32	22	22	30	30	25	19
NC	–	–	–	–	–	–	–	–

value of 37.3493 $\mu\text{g}/\text{mL}$, than the ZONP2 because of its comparatively larger surface area [55].

Antibacterial activity: The antimicrobial activity of ZONPs was evaluated by the disc diffusion method using *B. cereus* (MTCC 430) and *S. aureus* (MTCC 3160) as Gram-positive strains, and *K. pneumoniae* (MTCC 109) and *V. cholerae* (MTCC 3906) as Gram-negative strains, with ciprofloxacin (5 μg) used as the positive control. The values were tabulated in Table-3. The negative control showed no inhibition zone, while ZONP1 exhibited broad-spectrum antibacterial activity against both Gram-positive and Gram-negative strains with a dose-dependent increase. In contrast, ZONP2 showed dose-dependent activity primarily against Gram-positive *B. cereus*, with a maximum inhibition zone of 25 mm, which may be attributed to oxygen vacancies enhancing ROS generation; the improved biological activity compared to chemically synthesized ZnO nanoparticles is mainly due to surface-bound biomolecules that damage microbial cell walls and lead to cell death [50,56-58].

Conclusion

In summary, zinc oxide nanoparticles were successfully synthesized using *A. altalis* plant extracts and exhibited effective antimicrobial activity at higher concentrations. The formation of crystalline, biomolecule-capped nanoparticles was confirmed by XRD, FTIR and UV-Vis analyses, while SEM revealed agglomerated morphology and EDS verified elemental composition. The nanoparticles showed appreciable surface area and pore size, along with moderate to good antibacterial, anti-inflammatory, and antioxidant activities, attributed to bioactive capping agents that stabilize ROS and enhance functional performance. Further studies involving metal or non-metal doping, particle size distribution analysis, and cytotoxicity evaluation on normal cells are recommended to improve the properties, applicability, and safety of these green-synthesized nanoparticles.

ACKNOWLEDGEMENTS

The authors are thankful to Department of Chemistry, Women's Christian College, Nagercoil and Sree Ayyappa College for Women, Chunkankadai for providing facilities to conduct the research. The authors also thankful to the Instrumentation Centres of Alagappa University, Calicut University, SAIF-CUSAT, CSIR-CECRI and BIOMEITEZ Nagercoil, India for providing support in characterization.

CONFLICT OF INTEREST

The authors declare that there is no conflict of interests regarding the publication of this article.

DECLARATION OF AI-ASSISTED TECHNOLOGIES

During the preparation of this manuscript, the authors used an AI-assisted tool(s) to improve the language. The authors reviewed and edited the content and take full responsibility for the published work.

REFERENCES

- M. Mardani-Talae, J. Razmjou, A. Ajdari, J.E. Serrão and P. Vivekanandhan, *Sci. Rep.*, **15**, 13596 (2025); <https://doi.org/10.1038/s41598-025-97535-w>
- J. Nandhini, E. Karthikeyan and S. Rajeshkumar, *Resour. Chem. Mater.*, **3**, 294 (2024); <https://doi.org/10.1016/j.recm.2024.05.001>
- A.A. Al-Askar, A.H. Hashem, N.I. Elhussieny and E. Saied, *Molecules*, **28**, 4679 (2023); <https://doi.org/10.3390/molecules28124679>
- I. Ravhudzulo, M.S. Mthana, M.C. Ogwegbu, K. Ramachela, D.M.N. Mthiyane and D.C. Onwudiwe, *Discover Appl. Sci.*, **7**, 293 (2025); <https://doi.org/10.1007/s42452-025-06728-5>
- S. Saleem, M.H. Jameel, N. Akhtar, N. Nazir, A. Ali, A. Zaman, A. Rehman, S. Butt, F. Sultana, M. Mushtaq, J.H. Zeng, M. Amami and K. Althubeiti, *Arab. J. Chem.*, **15**, 103518 (2022); <https://doi.org/10.1016/j.arabj.2021.103518>
- B. Naiel, M. Fawzy, M.W.A. Halmy and A.E.D. Mahmoud, *Sci. Rep.*, **12**, 20370 (2022); <https://doi.org/10.1038/s41598-022-24805-2>
- H.S. Han, J.S. Jung, Y.-I. Jeong and K.C. Choi, *Materials*, **16**, 6669 (2023); <https://doi.org/10.3390/ma16206669>
- M.A. Shabbir, M. Naveed, S. Rehman, N. Ain, T. Aziz, M. Alharbi, A. Alsahammari and A.F. Alasmari, *ACS Omega*, **8**, 33358 (2023); <https://doi.org/10.1021/acsomega.3c02744>
- A. Singh, N.B. Singh, I. Hussain, H. Singh, V. Yadav and S.C. Singh, *J. Biotechnol.*, **233**, 84 (2016); <https://doi.org/10.1016/j.jbiotec.2016.07.010>
- S. Shrestha, L. Tiwari, S. Dhungana, J. Maharjan, D. Khadka, A.A. Kim, M.R. Pokhrel, J. Baral, M. Park and B.R. Poudel, *Nanomaterials*, **15**, 858 (2025); <https://doi.org/10.3390/nano15110858>
- M.W. Mazhar, M. Ishtiaq, M. Maqbool, A. Arshad, M.A. Alshehri, S.S. Alhelaify, O.M. Alharthy, M. Shukry and S.M. Sayed, *Sci. Rep.*, **14**, 24671 (2024); <https://doi.org/10.1038/s41598-024-74163-4>
- S. Fakhari, M. Jamzad and H. Kabiri Fard, *Green Chem. Lett. Rev.*, **12**, 19 (2019); <https://doi.org/10.1080/17518253.2018.1547925>
- M. Naseer, U. Aslam, B. Khalid and B. Chen, *Sci. Rep.*, **10**, 9055 (2020); <https://doi.org/10.1038/s41598-020-65949-3>
- D. Purushotham, A. Mavinakere Ramesh, D. Shetty Thimmappa, N. Kalegowda, G. Hittanahallikoppal Gajendramurthy, S.P. Kollur and M. Mahadevamurthy, *Int. J. Mol. Sci.*, **26**, 4739 (2025); <https://doi.org/10.3390/ijms26104739>
- A. Jayachandran, T.R. Awasthy and A.S. Nair, *Biochem. Biophys. Rep.*, **26**, 100995 (2021); <https://doi.org/10.1016/j.bbrep.2021.100995>
- A.E. Alprol, A. Eleryan, A. Abouelwafa, A.M. Gad and T.M. Hamad, *Sci. Rep.*, **14**, 32160 (2024); <https://doi.org/10.1038/s41598-024-80757-9>
- O.O. Oluwaniyi and B.T. Oyewo, *Nano Select*, **6**, e202400110 (2025); <https://doi.org/10.1002/nano.202400110>
- M.Y. Al-darwesh, S.S. Ibrahim and M.A. Mohammed, *Results Chem.*, **7**, 101368 (2024); <https://doi.org/10.1016/j.rechem.2024.101368>
- B. Sumanth, T.R. Lakshmeesha, M.A. Ansari, M.A. Alzohairy, A.C. Udayashankar, B. Shobha, S.R. Niranjana, C. Srinivas and A. Almatroudi, *Int. J. Nanomedicine*, **15**, 8519 (2020); <https://doi.org/10.2147/IJN.S271743>
- M.M. Chikkanna, S.E. Neelagund and K.K. Rajashekarappa, *SN Appl. Sci.*, **1**, 117 (2019); <https://doi.org/10.1007/s42452-018-0095-7>
- H. Agarwal, S. Venkat Kumar and S. Rajeshkumar, *Resour. Effic. Technol.*, **3**, 406 (2017); <https://doi.org/10.1016/j.reffit.2017.03.002>
- N. Bala, S. Saha, M. Chakraborty, M. Maiti, S. Das, R. Basu and P. Nandy, *RSC Adv.*, **5**, 4993 (2015); <https://doi.org/10.1039/C4RA12784F>
- S. Faisal, H. Jan, S.A. Shah, S. Shah, A. Khan, M.T. Akbar, M. Rizwan, F. Jan, N. Wajidullah, N. Akhtar, A. Khattak and S. Syed, *ACS Omega*, **6**, 9709 (2021); <https://doi.org/10.1021/acsomega.1c00310>
- M. Aliannezhadi, F. Doost Mohamadi, M. Jamali and F. Shariatmadar Tehrani, *Sci. Rep.*, **15**, 7203 (2025); <https://doi.org/10.1038/s41598-025-90305-8>
- E. Tilahun, Y. Adimasu and Y. Dessie, *ACS Omega*, **8**, 27344 (2023); <https://doi.org/10.1021/acsomega.3c02709>
- Y.H.I. Mohammed, S. Alghamdi, B. Jabbar, D. Marghani, S. Beigh, A.S. Abouzied, N.E. Khalifa, W.M.A. Khojali, B. Huwaimel, D.H.M. Alkhalifah and W.N. Hozzein, *ACS Omega*, **8**, 32027 (2023); <https://doi.org/10.1021/acsomega.3c03908>
- A. Umamaheswari, S.L. Prabu, S.A. John and A. Puratchikody, *Biotechnol. Rep.*, **29**, e00595 (2021); <https://doi.org/10.1016/j.btre.2021.e00595>
- S. Maher, S. Nisar, S.M. Aslam, F. Saleem, F. Behlil, M. Imran, M.A. Assiri, A. Nouroz, N. Naheed, Z.A. Khan and P. Aslam, *ACS Omega*, **8**, 15920 (2023); <https://doi.org/10.1021/acsomega.2c07621>
- K.R.M. Swamy, *Int. J. Dev. Res.*, **14**, 66175 (2024).
- M.S. Sikarwar, B.J. Hui, K. Subramaniam, B.D. Valeisamy, L. Kar Yean and K. Balaji, *J. Appl. Pharm. Sci.*, **5**, 94 (2015); <https://doi.org/10.7324/JAPS.2015.50518>
- C. Pradhan, M. Mohanty and A. Rout, *Front. Life Sci.*, **6**, 71 (2012); <https://doi.org/10.1080/21553769.2013.765811>
- F. Fitrya, E. Elfita, S.F. Ferlinahayati, S.F. Septami, U.T. Sabrina, F.S. Wahyuni, A. Amriani and R.P. Novita, *Phytomed. Plus*, **5**, 100696 (2025); <https://doi.org/10.1016/j.phyplu.2024.100696>
- K.A. Mehta, Y.C.R. Quek and C.J. Henry, *Front. Nutr.*, **10**, 1156155 (2023); <https://doi.org/10.3389/fnut.2023.1156155>
- A. Aladesanmi, A.J. Adetunji, O. Odiba, E. Ogu, O. Odeiran, S.A. Akintunde, O. Oriola and A. Olubunmi, *Afr. J. Infect. Dis.*, **16S2**, 33 (2022); <https://doi.org/10.21010/Ajid.v16i2S.5>
- F. Rahman, M.A. Majed Patwary, M.A. Bakar Siddique, M.S. Bashar, M.A. Haque, B. Akter, R. Rashid, M.A. Haque and A.K.M. Royhan Uddin, *R. Soc. Open Sci.*, **9**, 220858 (2022); <https://doi.org/10.1098/rsos.220858>
- K. Verma, S. Ghosh, N. Pradeep and S.G.A. Manuel, *Int. J. Adv. Res.*, **9**, 394 (2021); <https://doi.org/10.21474/IJAR01/13027>
- C. Aydin Acar, M.A. Gencer, S. Pehlivanoglu, S. Yesilot and S. Donmez, *Int. Wound J.*, **21**, e14413 (2024); <https://doi.org/10.1111/iwj.14413>
- S. Kulkarni, H.N. Akolkar, V.M. Khedkar, R. Ramasamy, K.R. Mahanwar and N.R. Darekar, *Biogenic-Based Metal Nanomaterials for Sustainable Engineering Applications*, Apple Academic Press, New York (2025).
- Y.A. Selim, M.A. Azb, I. Ragab and M. H. M. Abd El-Aziz, *Sci. Rep.*, **10**, 3445 (2020); <https://doi.org/10.1038/s41598-020-60541-1>
- M.C. Walker and J. K. Gierse, in eds.: S. Ayoub, R. Flower and M. Seed, *In Vitro Assays for Cyclooxygenase Activity and Inhibitor Characterisation*, Humana Press, pp. 131-144 (2010).
- B. Axelrod, T. M. Cheesbrough and S. Laakso, *Methods Enzymol.*, **71**, pp. 441-451 (1981); [https://doi.org/10.1016/0076-6879\(81\)71055-3](https://doi.org/10.1016/0076-6879(81)71055-3)
- N. Asif, M. Amir and T. Fatma, *Bioprocess Biosyst. Eng.*, **46**, 1377 (2023); <https://doi.org/10.1007/s00449-023-02886-1>

43. T. Bizuayehu, B. Kassaw and M. Kendie, *Results Chem.*, **13**, 102046 (2025); <https://doi.org/10.1016/j.rechem.2025.102046>
44. C.C. Singh, G.D. Gena, T. Rajesh, C.S. Biju, S.J. Dhas, S. Aswathappa and A.I. Almansour, *J. Mol. Struct.*, **1322**, 140293 (2025); <https://doi.org/10.1016/j.molstruc.2024.140293>
45. S. Meneceur, H. Hemmami, A. Bouafia, S.E. Laouini, M.L. Tedjani, D. Berra and M.S. Mahboub, *Biomass Convers. Biorefin.*, **14**, 5357 (2024); <https://doi.org/10.1007/s13399-022-02734-4>
46. Ö. Erdoğan, S. Paşa, G.M. Demirbolat, F. Birtekocak, M. Abbak and Ö. Çevik, *Inorganic and Nano-Metal Chemistry*, **55**, 67 (2025); <https://doi.org/10.1080/24701556.2023.2240768>
47. A.K. Khajuria, A. Kandwal, R.K. Sharma, R.K. Bachheti, L.A. Worku and A. Bachheti, *Sci. Rep.*, **15**, 6541 (2025); <https://doi.org/10.1038/s41598-025-85264-z>
48. P. Ramesh, K. Saravanan, P. Manogar, J. Johnson, E. Vinoth and M. Mayakannan, *Sens. Biosensing Res.*, **31**, 100399 (2021); <https://doi.org/10.1016/j.sbsr.2021.100399>
49. S.E. Dafalla, N.A. Aldabaan, U.M. Muddapur, S. Angadi, L.R. Patil, I.A. Shaikh, A.A. Khan, S.M.S. Iqbal, A.R. Shet, S.V. Desai and V.S. Hombalimath, *J. Umm Al-Qura Univ. Appl. Sci.*, **11**, 308 (2025); <https://doi.org/10.1007/s43994-024-00161-x>
50. J. Nandhini, E. Karthikeyan, M. Sheela, M. Bellarmin, B. Gokula Kannan, A. Pavithra, D. Sowmya Sri, S. Siva Prakash and S. Rajesh Kumar, *Intelligent Pharmacy*, **3**, 90 (2025); <https://doi.org/10.1016/j.ipha.2024.09.003>
51. A. Husen and M. Iqbal, *Nanomaterials and Plant Potential*, Springer International Publishing, Cham (2019).
52. A.R. Maheo, B.S.M. Vithiya and T.A.A. Prasad, *Results Surf. Interf.*, **6**, 100048 (2022); <https://doi.org/10.1016/j.rsurfi.2022.100048>
53. A.K.M.S. Islam, R. Bhuiyan, M.A.I. Khan, S. Akter, M.R. Islam, M.A.R. Khokon and M.A. Latif, *Appl. Biochem. Biotechnol.*, **197**, 587 (2025); <https://doi.org/10.1007/s12010-024-05020-3>
54. C.A. Mbachu, A.K. Babayemi, T.C. Egbosiuba, J.I. Ike, I.J. Ani and S. Mustapha, *Results Eng.*, **19**, 101198 (2023); <https://doi.org/10.1016/j.rineng.2023.101198>
55. K. Fatima, M. Asif, U. Farooq, S.J. Gilani, M.N. Bin Jumah and M.M. Ahmed, *ACS Omega*, **9**, 15882 (2024); <https://doi.org/10.1021/acsomega.3c08143>
56. S.A. Akintelu and A.S. Folorunso, *Bionanoscience*, **10**, 848 (2020); <https://doi.org/10.1007/s12668-020-00774-6>
57. P.K. Upadhyay, V.K. Jain, S. Sharma, A.K. Shrivastav and R. Sharma in *IOP Conf. Ser. Mater. Sci. Eng.*, **798**, 012025 (2020);
58. A.S. Abdelbaky, A.M.H.A. Mohamed, M. Sharaky, N.A. Mohamed and Y.M. Diab, *Chem. Biol. Technol. Agric.*, **10**, 63 (2023); <https://doi.org/10.1186/s40538-023-00432-5>